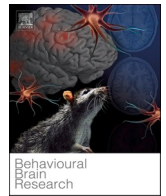


Contents lists available at [ScienceDirect](https://www.sciencedirect.com)

Behavioural Brain Research

journal homepage: [www.elsevier.com/locate/bbr](http://www.elsevier.com/locate/bbr)

Short communication

## Enhancing adult neurogenesis promotes contextual fear memory discrimination and activation of hippocampal-dorsolateral septal circuits

Antoine Besnard<sup>a,b,c</sup>, Amar Sahay<sup>a,b,c,d,\*</sup><sup>a</sup> Center for Regenerative Medicine, Massachusetts General Hospital, Boston, MA, 02114, USA<sup>b</sup> Harvard Stem Cell Institute, Cambridge, MA, 02138, USA<sup>c</sup> Department of Psychiatry, Massachusetts General Hospital, Harvard Medical School, Boston, MA, 02114, USA<sup>d</sup> BROAD Institute of Harvard and MIT, Cambridge, MA, 02142, USA

## ARTICLE INFO

## Keywords:

Adult neurogenesis

Dentate gyrus

CA3

Dorsolateral septum

c-Fos

Somatostatin

## ABSTRACT

Hippocampal circuitry is continuously modified by integration of adult-born dentate granule cells (DGCs). Prior work has shown that enhancing adult hippocampal neurogenesis decreases interference or overlap or conflict between ensembles of similar contexts and promotes discrimination of a shock-associated context from a similar, neutral context. However, the impact of enhanced integration of adult-born neurons on hippocampal network activity or downstream circuits such as the dorsolateral septum that mediate defensive behavioral responses is poorly understood. Here, we first replicated our finding that genetic expansion of the population of adult-born dentate granule cells (8 weeks and younger) promotes contextual fear discrimination. We found that enhanced contextual fear discrimination is associated with greater c-Fos expression in discrete hippocampal subfields along the proximo-distal and dorsoventral axis. Examination of the dorsolateral septum revealed an increase in activation of somatostatin expressing neurons consistent with recent characterization of these cells as calibrators of defensive behavior. Together, these findings begin to shed light on how genetically enhancing adult hippocampal neurogenesis affects activity of hippocampal-dorsolateral septal circuits.

## 1. Introduction

Adult-born dentate granule cells (DGCs) are continuously generated from neural stem cells in the hippocampal dentate gyrus (DG) in humans and rodents throughout life [1–6]. Adult-born DGCs functionally integrate into hippocampal circuitry and exhibit heightened synaptic and structural plasticity during distinct stages of maturation [5,7–10]. Consistent with proposed functions of DG in pattern separation, a circuit mechanism by which similar inputs are made divergent at the level of output [5,11–20], adult-born DGCs have been implicated in resolution of memory interference in a range of behavioral paradigms -spatial learning, contextual fear learning, delayed non-match to place radial arm maze, and object displacement on touch screen [5]. A causal role for adult hippocampal neurogenesis in mediating contextual fear discrimination has been demonstrated using gain of function [21–24] and loss of function genetic approaches [25]. While in vivo calcium imaging suggests that 6-week-old adult-born DGCs encode contextual information [26], how adult-born DGCs resolve memory interference at a circuit level is poorly understood. Cellular imaging studies using immediate

early genes suggest that adult-born DGCs may promote discrimination between similar contexts by influencing population activity in the dorsal and ventral DG [22] and in CA3 [27]. Much work remains to be done to understand how modulating levels of adult hippocampal neurogenesis affects hippocampal circuits and key outputs that mediate contextual memory discrimination.

The hippocampus is defined by distinct patterns of afferent and efferent connectivity along its dorsoventral axis [28–30]. The dorsal (or septal) hippocampus is thought to mediate the encoding of contextual information [31,32]. The ventral (or temporal) hippocampus processes information underlying goals [32–34]. The DG can be divided into the supra and infrapyramidal blades receiving a gradient of inputs proceeding from the lateral and medial entorhinal cortex [35–37]. Molecular and functional heterogeneity along the proximodistal axis of CA3 [14,38], CA2 [39] and CA1 [40–42] may differentially relay hippocampal information to downstream subcortical circuits to calibrate fear responses [43]

The DLS is a major subcortical target of the hippocampus that mediates contextual gating of defensive behavioral responses [44,45]. We

\* Corresponding author.

E-mail address: [asahay@mgh.harvard.edu](mailto:asahay@mgh.harvard.edu) (A. Sahay).<https://doi.org/10.1016/j.bbr.2020.112917>

Received 4 August 2020; Received in revised form 1 September 2020; Accepted 9 September 2020

Available online 16 September 2020

0166-4328/© 2020 Elsevier B.V. All rights reserved.

recently demonstrated that contextual discrimination involves CA3 projections to CA1 and the dorsolateral septum (DLS). Dorsal CA3 projections to CA1 and DLS control defensive behavioral responses (freezing behavior) in a context associated with a footshock and a similar neutral context, respectively [46]. Ventral CA3 projections to CA1 and DLS can promote or attenuate defensive responses in a context agnostic manner, respectively [46]. Within DLS, somatostatin-expressing neurons (SST) receive monosynaptic inputs from hippocampal CA3 and these SST inhibitory neurons calibrate freezing behavior [45].

Here, we assessed the impact of inducible enhancement of adult neurogenesis on DG-CA3-CA1 activity along the proximo-distal and dorsal-ventral axes and recruitment of the DLS during contextual fear discrimination. We first confirmed that enhancing levels of neurogenesis is sufficient to improve contextual fear discrimination. We found that enhanced contextual fear discrimination is associated with greater c-Fos expression in discrete hippocampal subfields along the proximo-distal and dorsoventral axes and recruited activation of DLS SST-expressing neurons. Together, these data begin to identify how genetically enhancing neurogenesis impacts hippocampal-DLS network activity to support contextual fear discrimination.

## 2. Results

### 2.1. Genetically enhancing adult hippocampal neurogenesis promotes contextual fear discrimination

Our prior work showed that mice with genetically enhanced neurogenesis perform better in a contextual fear discrimination paradigm. We sought to determine if this finding was reproducible using a different inducible Cre driver line (Nestin-CreER<sup>T2</sup>) [47–49] from the one used previously [21,50] to recombine the pro-apoptotic gene *Bax* in neural

stem cells and progenitors in the adult DG (Nestin-CreER<sup>T2</sup>::*Bax*<sup>f/f</sup> mice Fig. 1A). 8 weeks following tamoxifen-induced recombination of *Bax* in adult neural stem cells, we performed behavioral testing of mice in an abbreviated version of the contextual fear conditioning discrimination learning (CFCDL) task (Fig. 1B–C). Mice were then perfused for analysis of neurogenesis by DCX immunostaining and network activity by c-Fos immunostaining. Tamoxifen-treated Nestin-CreER<sup>T2</sup>::*Bax*<sup>f/f</sup> mice did not differ from controls during the first 3 days of conditioning (Fig. 1D) but exhibited better discrimination between context A and neutral similar context B or neutral distinct context C than vehicle-treated controls on day 4 (Fig. 1E–F).

### 2.2. Genetically enhancing adult hippocampal neurogenesis increases c-Fos expression in discrete hippocampal subfields following recall in similar, neutral context

Next, we evaluated the activity of different hippocampal subfields following exposure of Nestin-CreER<sup>T2</sup>::*Bax*<sup>f/f</sup> mice to similar, neutral context. At the end of the behavioral experiment (day 5), a subset of the vehicle and tamoxifen-treated mice (6 vehicle and 6 tamoxifen) were re-exposed to context B and sacrificed 60 min later (Fig. 1G). Another 3 mice were sacrificed in the home-cage (2 vehicle and 1 tamoxifen) and were used as no re-exposure control mice for DCX and c-Fos analysis. Mice-treated with tamoxifen (n = 6 retrieval in context B + 1 home cage control) displayed greater number of DCX positive cells compared to vehicle controls (n = 6 retrieval in context B + 2 home cage controls), preferentially in the intermediate and ventral part of DG (Fig. 1H–I). c-Fos is an immediate early gene whose expression is rapidly and transiently enhanced in response to neuronal activity [51]. c-Fos expression was assessed across different hippocampal subfields (DG, CA3 and CA1) along the dorsoventral axis (dorsal, intermediate and ventral) of the hippocampus (Fig. 2A–G). Exposure to context B elicited a robust

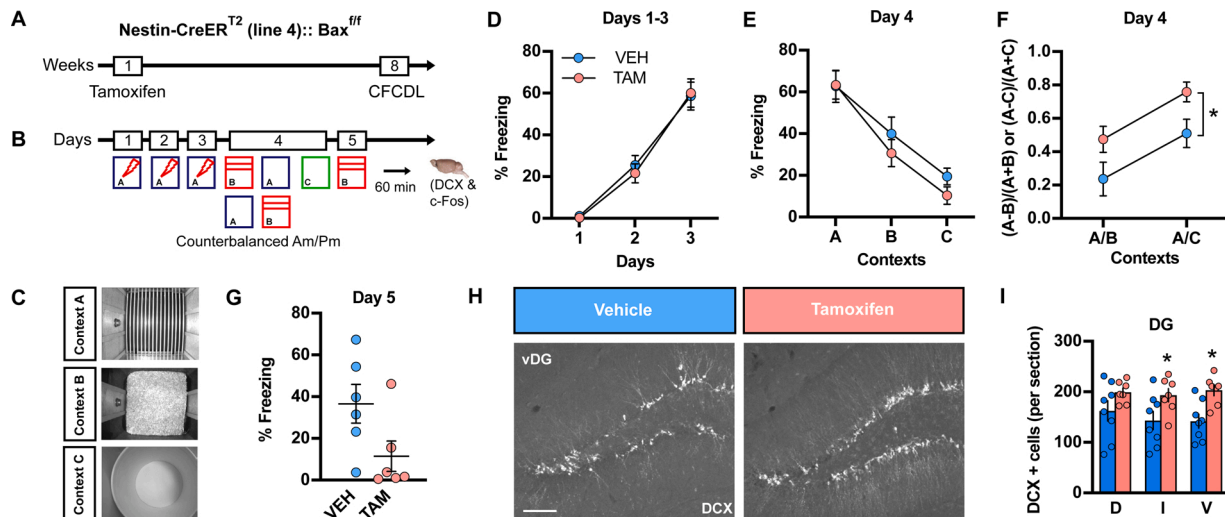


**Fig. 1.** Genetically enhancing adult hippocampal neurogenesis improves contextual fear discrimination.

**A)** Schematic illustrating the strategy employed to genetically enhance adult hippocampal neurogenesis levels in Nestin-CreER<sup>T2</sup>::*Bax*<sup>f/f</sup> mice. **B)** CFCDL consisted of 3 days of training in context A and a single discrimination test on day 4. At the end of testing, a subset of the mice were re-exposed to context B 60 min prior to sacrifice for DCX and c-Fos analysis. **C)** Contexts A, B and C employed for CFCDL procedure in which mice were trained to discriminate between context A associated with a mild footshock and neutral similar and distinct contexts B and C. **D)** No difference in acquisition of CFC. Data (means  $\pm$  SEM; n = 16, 15 mice per group) were analyzed using mixed factor two-way ANOVA (repeated measure over time) (detailed in Supplementary Table 1), no significant difference. **E–F)** Tamoxifen-treated mice exhibited increased contextual fear discrimination (A vs B and A vs C) as demonstrated by the increase in discrimination ratio on day 4 (F). Data (means  $\pm$  SEM; n = 16, 15 mice per group) were analyzed using mixed factor two-way ANOVA (repeated measure over time), for discrimination ratio (F): main effect of context  $F_{(1,29)} = 23.80$ ,  $p < 0.0001$ ; main effect of treatment,  $F_{(1,29)} = 5.649$ ,  $p < 0.05$ ; context  $\times$  treatment  $F_{(1,29)} = 0.008$ , NS; (detailed in Supplementary Table 1). **G)** Freezing behavior of vehicle and tamoxifen-treated mice 60 min prior to sacrifice for subsequent c-Fos analysis. Data (means  $\pm$  SEM; n = 6, 6 mice per group) were analyzed using unpaired Student two-tailed T-test (detailed in Supplementary Table 1), no significant difference. **H)** Immunohistochemistry for doublecortin (DCX) in the DG of Nestin-CreER<sup>T2</sup>::*Bax*<sup>f/f</sup> mice-treated with vehicle or Tamoxifen. Representative images for 8, 7 independent animals per group. Scale bar: 100  $\mu$ m. **I)** Quantification of DCX positive cells in the DG of vehicle and tamoxifen-treated mice. Data (means  $\pm$  SEM; n = 8, 7 mice per group) were analyzed with unpaired Student two-tailed T-test, for vDG:  $t = 3.451$ ,  $df = 13$ ;  $p < 0.01$  (detailed in Supplementary Table 1), \* $p < 0.05$ , tamoxifen versus vehicle.

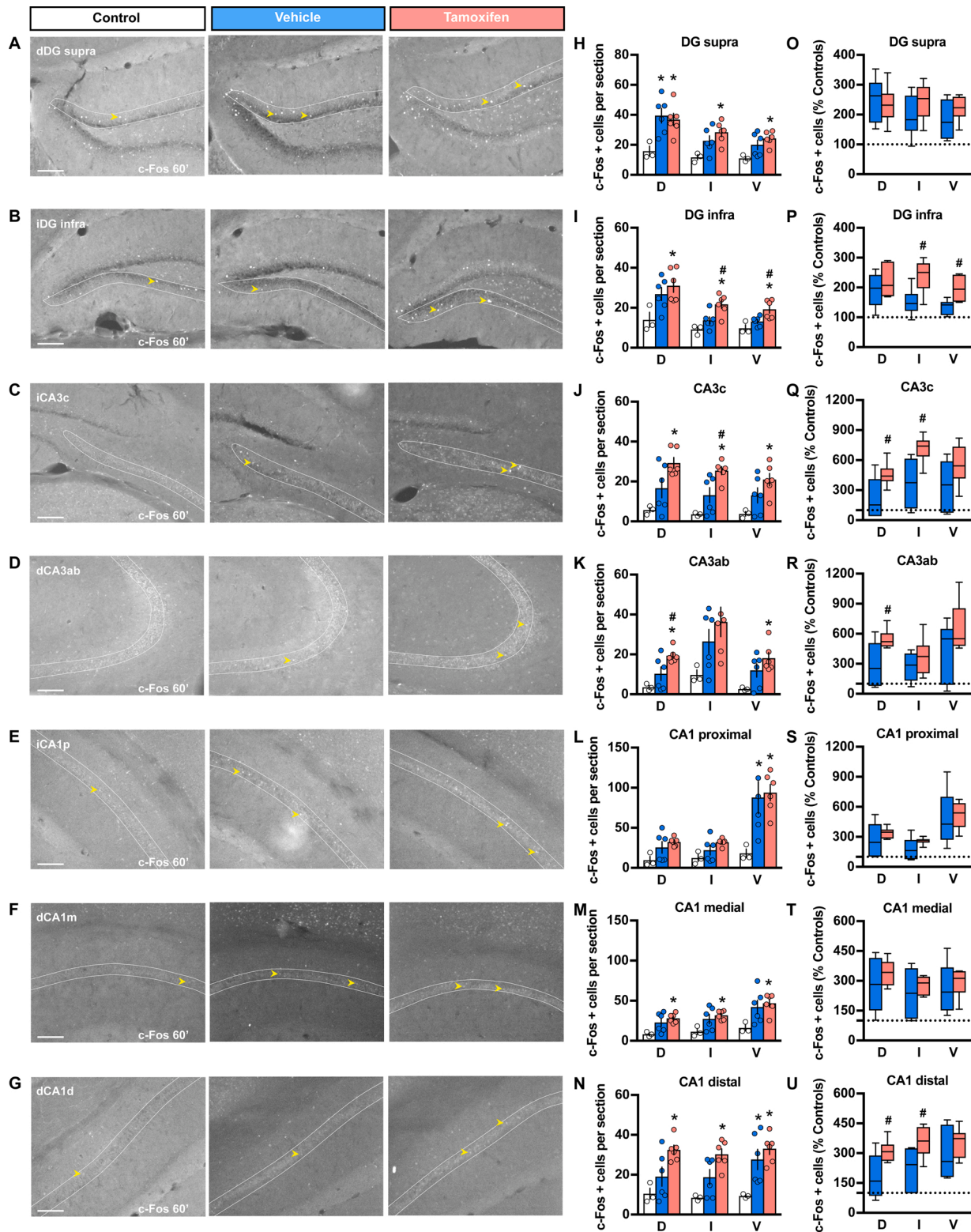


**Fig. 2.** Enhancing adult hippocampal neurogenesis modulates c-Fos expression in discrete hippocampal subfields following contextual fear discrimination. **A-G)** Immunohistochemistry for c-Fos (yellow arrowheads) in the DG (A,B), CA3 (C,D) and CA1 (E,F,G) of home cage controls, vehicle and tamoxifen-treated animals 60 min following exposure to context B. Representative images for 3, 6, 6 independent animals per group. Scale bars: 100  $\mu$ m. **H-N)** Quantifications of c-Fos + cells in the dorsal, intermediate and ventral DG (H,I), CA3 (J,K), and CA1 (L-N) for home cage controls, vehicle and tamoxifen-treated animals 60 min following exposure to context B. Data (means  $\pm$  SEM;  $n = 3, 6, 6$  mice per group) were analyzed using one-way ANOVA followed by Tukey's multiple comparisons post-hoc test (detailed in Supplementary Table 1), \* $p < 0.05$ , vehicle or tamoxifen versus control, # $p < 0.05$ , tamoxifen versus vehicle. **O-U)** Quantifications of c-Fos + cells expressed as a percent controls in the dorsal, intermediate and ventral DG (O,P), CA3 (Q,R), and CA1 (S-U) for vehicle and tamoxifen-treated animals. Data (means  $\pm$  SEM;  $n = 6, 6$  mice per group) were analyzed using unpaired Student two-tailed T-test (detailed in Supplementary Table 1), # $p < 0.05$ , tamoxifen versus vehicle.

increase in c-Fos expression (in both vehicle and tamoxifen-treated mice) in ventral CA1 (proximal and distal) (Fig. 2L,N). Tamoxifen-treated mice displayed an increase in c-Fos expression in DG inferior blade (Fig. 2I,P), intermediate and dorsal CA3c (Fig. 2J,Q), dorsal CA3ab (Fig. 2K,R), and intermediate and dorsal distal CA1 (Fig. 2N,U).

### 2.3. Genetically enhancing adult hippocampal neurogenesis enhances c-Fos expression within DLS SST-expressing neurons following recall in similar, neutral context

We have recently demonstrated that CA3 projections to DLS control the activity of SST-expressing neurons that modulate contextual fear responses in mice [45,46]. We therefore asked how facilitating contextual fear discrimination by enhancing levels of hippocampal neurogenesis alters the activity DLS SST-expressing neurons. Exposure to context B elicited an increase in c-Fos expression in the medial and

lateral aspects of DLS (Fig. 3A-B). Tamoxifen-treated mice displayed an increase in c-Fos expression in the lateral part of DLS, as compared to vehicle treated-mice (Fig. 3C). Further, we evaluated c-Fos expression levels in SST-expressing cells in the lateral part of DLS (Fig. 3D-E) and found greater c-Fos expression in tamoxifen-treated mice (Fig. 3F-G).

### 3. Discussion

It is important to assess reproducibility of adult hippocampal neurogenesis associated phenotypes using different inducible driver lines that target adult neural stem cells and progenitors. We previously reported that enhancing levels of hippocampal neurogenesis was sufficient to facilitate contextual fear discrimination [21]. In the present work, we used a distinct Nestin-CreER<sup>T2</sup> mouse line that exclusively targets neural stem cells and progenitors in the adult SVZ and SGZ [47]. We found an increase in hippocampal neurogenesis, which was much less pronounced relative to our previous report using a different driver line [21].

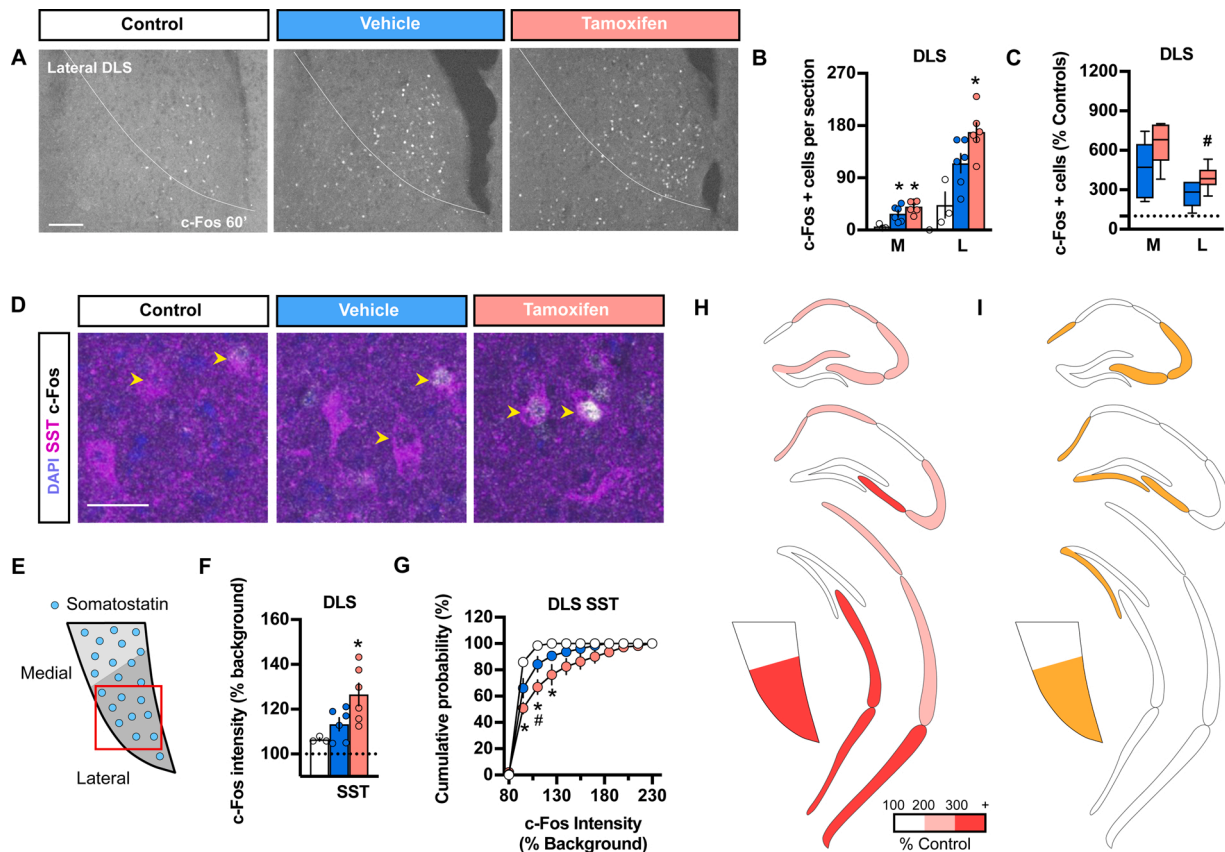


**Fig. 3.** Enhancing adult hippocampal neurogenesis increases activity of DLS SST-expressing neurons following contextual fear discrimination.

**A)** Immunohistochemistry for c-Fos in the DLS of home cage controls, vehicle and tamoxifen-treated animals 60 min following exposure to context B. Representative images for 3, 6, 6 independent animals per group. Scale bar: 100  $\mu$ m. **B)** Quantifications of c-Fos + cells in the medial and lateral regions of DLS for home cage controls, vehicle and tamoxifen-treated animals 60 min following exposure to context B. Data (means  $\pm$  SEM; n = 3, 6, 6 mice per group) were analyzed using one-way ANOVA followed by Tukey's multiple comparisons post-hoc test (detailed in Supplementary Table 1), \*p < 0.05, vehicle or tamoxifen versus control. **C)** Quantifications of c-Fos + cells expressed as a percent of controls in the medial and lateral parts of DLS for vehicle and tamoxifen-treated animals. Data (means  $\pm$  SEM; n = 6, 6 mice per group) were analyzed using unpaired Student two-tailed T-test, for lateral DLS: t = 2.328, df = 10; p < 0.05 (detailed in Supplementary Table 1), #p < 0.05, tamoxifen versus vehicle. **D)** Immunohistochemistry for SST and c-Fos (yellow arrowheads) in home cage controls, vehicle and tamoxifen-treated animals. Nuclei are counterstained with DAPI. Representative images for 3, 6, 6 independent animals per group. Scale bar: 25  $\mu$ m. **E)** c-Fos expression was measured in SST-expressing neurons localized in the lateral part of DLS (red box). **F)** Tamoxifen-treated animals showed greater overall expression of c-Fos in SST-expressing neurons as compared to controls animals. Data (means  $\pm$  SEM; n = 3, 6, 6 mice per group) were analyzed using one-way ANOVA followed by Tukey's multiple comparisons post-hoc test (detailed in Supplementary Table 1), \*p < 0.05, tamoxifen versus control. **G)** Analysis of c-Fos levels in SST-expressing neurons revealed varying levels of c-Fos expression in subsets of cells and revealed a significant increase in c-Fos expression in tamoxifen-treated mice compared to controls and vehicle-treated animals. Data (means  $\pm$  SEM; n = 3, 6, 6 mice per group) were analyzed using mixed factor two-way ANOVA (repeated measure over time) main effect of intensity  $F_{(10,120)} = 231.3$ , p < 0.0001; main effect of treatment,  $F_{(2,12)} = 6.216$ , p < 0.05; intensity x treatment  $F_{(20,120)} = 3.599$ , p < 0.0001 followed by Bonferroni's multiple comparisons post-hoc test (detailed in Supplementary Table 1), \*p < 0.05, tamoxifen versus control, #p < 0.05, tamoxifen versus vehicle. **H-I)** Summary of relative c-Fos expression along the dorsoventral axis of the hippocampus and the dorsolateral septum. Color codes depict the relative increase of c-Fos expression in vehicle-treated mice as a percent of controls (H) and statistical differences between vehicle and tamoxifen-treated animals (I).

Here, the increase in DCX expressing cells was more pronounced in intermediate and ventral DG, as opposed to the original mouse line where we observed an increase along the entire dorsoventral axis DG [52]. Preliminary studies indicated that higher doses of tamoxifen were required to yield a significant increase in DCX positive cells (180 mg/kg compared to 100 mg/kg in the original study, data not shown). In addition, mice were perfused following contextual fear discrimination learning as compared to naïve mice examined in the original study [21]. Nevertheless, we reproduced our previous observation demonstrating that an enhancement of adult hippocampal neurogenesis is sufficient to facilitate contextual fear discrimination.

We recently showed that CA3 projections to CA1 and dorsolateral septum (DLS) differentially contribute to contextual fear discrimination along the dorsoventral axis of the hippocampus [46]. While dorsal CA3 projections control defensive responses (freezing) in a context specific manner, ventral CA3 projections can bidirectionally control defensive responses in a context independent manner [46]. One mechanism by which ventral CA3 projections may attenuate freezing is via the recruitment of SST-expressing neurons in DLS [46]. This is relevant because optogenetic control of SST-expressing neurons in DLS appear to attenuate contextual fear responses [45]. In vivo calcium imaging of SST-expressing neurons in DLS demonstrated that these neurons are preferentially active during non-freezing events in a context associated with a footshock [45]. In the present work we attempted to evaluate hippocampal network and DLS SST activity in mice with enhanced neurogenesis following exposure to a similar, neutral context.

We recently demonstrated that efficient contextual fear discrimination is associated with greater c-Fos expression levels in DG (including both the superior and inferior blades) along the dorsoventral axis [45]. Herein, we found enhanced contextual fear discrimination was associated with higher c-Fos expression levels within the inferior blade of the ventral DG of mice with enhanced neurogenesis. Interestingly, a recent report found that adult-born neurons differentially control the excitability of DG mature granule cells in the inferior and superior blades [37]. Specifically, adult-born neurons promote the excitability of the granule cells in the inferior blade by modulating the synaptic strength of the medial entorhinal inputs. Conversely, they attenuate the excitability of the granule cells in the superior blade by modulating the synaptic strength of the lateral entorhinal inputs [37]. In this regard, it is noteworthy that the medial and lateral entorhinal inputs preferentially innervate ventral DG and dorsal DG, respectively [53,54]. This observation may explain how enhancing levels of neurogenesis in ventral DG increases c-Fos expression in the inferior blade upon contextual fear discrimination.

Hippocampal area CA3 plays an important role in the acquisition of contextual fear [55]. CA3 is heterogeneous at the molecular and functional level along the dorsoventral axis [29,38,56]. Previous work has suggested that the ventral hippocampus may preferentially contribute to contextual generalization [57–60] and we recently showed that dorsal and ventral CA3 differentially contribute to contextual fear discrimination [46]. While dorsal CA3/CA2 may be well suited for the discrimination of social cues and contextual representations [31,46,61], ventral CA3 may recruit CA1 and DLS in an opposite manner to modulate fear generalization [46]. In addition, CA3 is heterogeneous at the molecular and functional level along the proximodistal axis [38,62]. Proximal CA3 (CA3c) circuitry may be an optimal substrate for context discrimination [63–65] given its involvement in pattern separation [14]. We recently demonstrated that efficient contextual fear discrimination is associated with greater c-Fos expression levels in dorsal and ventral CA3ab [45]. Here, enhanced contextual fear discrimination was associated with higher c-Fos expression levels in CA3c along the dorso-ventral axis and additionally, in dorsal CA3a and CA3b [43].

Our previous work suggested that ventral CA3 projections to DLS attenuate freezing behavior while projections to ventral CA1 promote freezing behavior [46]. Conversely, dorsal CA3ab (including CA2) projections to dorsal CA1 and DLS promote freezing in the context

associated with the footshock or the similar, neutral context, respectively [46]. CA1 is heterogeneous along the proximodistal axis [41], and proximal and distal CA1 receive prominent inputs from the medial and lateral entorhinal cortex [66,67]. In addition, proximal and distal CA1 receive prominent inputs from CA3ab and CA3c, respectively [67]. Proximal CA1 displays strongest spatial modulation [40] and is necessary for contextual fear recall, unlike distal CA1 [42]. In our previous study, we demonstrated that c-Fos expression in CA1 along the dorso-ventral axis is insensitive to efficient contextual fear discrimination [45]. Here, enhanced contextual fear discrimination was associated with higher c-Fos expression levels within distal CA1 in the dorsal hippocampus (which was not analyzed in our previous study). This observation could suggest that while DG suprapyramidal blade, distal CA3 and proximal CA1 are recruited during recall in the conditioned context [42], DG infrapyramidal blade, proximal CA3 and distal CA1 are recruited upon exposure to the similar, neutral context and that enhancing neurogenesis promotes activation of this network. In support of this interpretation, DGc in the infrapyramidal blade are thought to project primarily to proximal CA3 [68–70]. In addition, previous findings suggest that non-spatial representations elicit preferential expression of the immediate early gene *Arc* in proximal CA3 and distal CA1 [71].

We did not detect significant correlations between c-Fos levels in CA3c and SST expressing neurons in the lateral septum or freezing behavior (data not shown). However, we found a significant correlation between c-Fos levels in intermediate CA1 (distal) and SST expressing neurons in the lateral septum (data not shown). These correlations (and lack thereof) will need to be directly ascertained with causal interrogation of CA subfield projections to DLS SST expressing neurons.

Taken together, these results indicate that enhancing levels of neurogenesis facilitates contextual fear discrimination by recruiting discrete hippocampal circuits along the dorsoventral and proximodistal axes (Fig. 3H–I). One such circuit mechanism could be the recruitment of intermediate CA3c which projects onto SST-expressing neurons whose activity is sufficient to attenuate freezing behavior [45]. In addition, dorsal CA3c could recruit distal CA1 whose long-range projections target the medial aspect of DLS and play a role in contextual fear retrieval [72].

### 3.1. Limitations

It should be noted that this study relies mainly on c-Fos expression as a proxy for neuronal activity and at a single time-point. Importantly, c-Fos expressing cells display distinct firing properties as compared to non c-Fos expressing place cells during contextual memory encoding [43,73,74]. Thus, c-Fos expressing cells may not fully capture the diversity of active ensembles of hippocampal neurons upon recall. In addition, immediate early genes display distinct temporal patterns of expression in the DG upon contextual fear recall [75]. Another limitation in the interpretation of this data set is that we did not analyze c-Fos in mice exposed to context associated with the footshock. Because enhancing levels of neurogenesis only affected freezing behavior in the similar, neutral context and exposure to the neutral context increased c-Fos expression in the hippocampus and dorsolateral septum [45], we restricted our c-Fos analysis to mice exposed only to context B. Further studies relying on longitudinal in vivo electrophysiological recordings and calcium imaging will enable precise dissection of how neurogenesis affects dynamics of cellular recruitment in intra- and extra- hippocampal circuits during contextual fear discrimination.

## 4. Methods

### 4.1. Animal care

Male mice were housed four per cage in a 12 h (7:00 a.m. to 7:00 p.m.) light/dark colony room at 22 °C – 24 °C with ad libitum access to

food and water. Age-matched, male mice (3–4 months old) were used for behavioral experiments. Cage-mates were pseudo-randomly assigned to groups during virus injection. Behavioral experiments took place between 8:00 a.m. and 6:00 p.m. All animals were handled and experiments were conducted in accordance with procedures approved by the Institutional Animal Care and Use Committee at the Massachusetts General Hospital and Boston University in accordance with NIH guidelines.

#### 4.2. Mouse lines

iBax mice are homozygous for a loxP-flanked *Bax* allele [76], hemizygous for a Nestin-CreER<sup>T2</sup> (line 4) transgene [47], and maintained on a mixed C57BL/6 and 129/SvEv background. Tail DNA from all offspring was genotyped by PCR to detect the presence of each transgene separately. All experiments were conducted with 8–12 week old mice.

#### 4.3. Drug administration

Tamoxifen (TAM) was dissolved in a solution of corn oil (C8267, Sigma, St Louis, MO) and 10 % ethanol. iBax mice (8–10-week-old) received Tamoxifen (180 mg/kg, Sigma, St. Louis, MO), or the same volume of corn oil and ethanol (vehicle), intraperitoneally once per day for 5 consecutive days.

#### 4.4. Contextual fear conditioning discrimination learning

The conditioning chambers (18 × 18 × 30 cm) consisted of 2 clear Plexiglas walls and ceiling, 2 metal walls, and a stainless steel grid floor (Coulbourn Instruments, Whitehall, PA). The conditioning chambers were placed inside a ventilated, sound-dampening isolation cubicles and lit by house lights mounted on one wall (Coulbourn Instruments, Whitehall, PA). FreezeFrame and FreezeView softwares (Actimetrics, Wilmette, IL) were used for recording and analyzing freezing behavior, respectively. For the training context (designated A throughout), the cubicle door was closed, the fan and house light were on, a light cue was on, stainless-steel bars were exposed, silver wall panels were used and each conditioning chamber was cleaned with 70 % ethanol between each trial. Context B was a modified version of A by covering the stainless-steel bars with a solid floor covered with bedding, black wall panels were used (covering 30 % of total wall surface), 15 cm high curved green plastic inserts covered the bottom half of the walls, and the house fan and lights were turned off. The cubicle door was left ajar and white noise was delivered through built-in speakers for the duration of the testing. The bedding was changed between trials. Context C consisted in a disposable 2.4 L white paper bucket placed out of the cubicle in the same experimental room as contexts A and B.

The contextual fear conditioning protocol consisted in a single 2 s footshock of 0.7 mA which was delivered 180 s after placement of the mouse in the training context A. The mouse was taken out 20 s after termination of the footshock. This procedure was repeated for 3 days (24 h apart). On day 4, 50 % of the animals were first tested in context A or B in the morning and context B or A in the afternoon. In some instances, animals were also tested in context C, which took place after both exposures to contexts A and B. No footshocks were delivered during the test sessions. Mice were allowed to rest for 1–2 h between tests. Freezing behavior over the initial 180 s was used to assess discrimination between both contexts. The discrimination ratio was calculated as (freezing in training context - freezing in similar context) / (freezing in training context + freezing in similar context).

#### 4.5. Immunohistochemistry

Mice were anesthetized with ketamine and xylazine (100 and 3 mg/kg body weight, respectively) and transcardially perfused with PBS

(10 mM phosphate buffer saline, pH 7.5,) at 4 °C, followed by 4% paraformaldehyde in PBS at 4 °C. Brains were post-fixed overnight in the same solution at 4 °C, then cryoprotected in PBS sucrose (30 % w/v) and stored at 4 °C before freezing in OCT on dry ice. Coronal serial sections (35 μm) were obtained using a Leica cryostat in six matched sets. Sections were stored in PBS with 0.01 % sodium azide at 4 °C. On day 1, free-floating sections were rinsed three times for 10 min in 10 mM phosphate buffer saline (PBS), pH 7.5, followed by a permeabilization step 15 min in 0.2 % Triton X-100 in PBS. The sections were rinsed another three times for 10 min in PBS and 2 h with a blocking buffer (10 % natural donkey serum (NDS; w/v)). After three rinses in PBS, incubation with primary antibodies rabbit anti c-fos, Santa Cruz SC52, 1:2,000 (Antibodyregistry.org: AB\_2106783)(discontinued); goat anti-SST, Santa Cruz SC7819, 1:400 (Antibodyregistry.org: AB\_2302603) (discontinued); goat anti-DCX, Santa Cruz SC8066, 1:1000 (Antibodyregistry.org: AB\_2088494) was carried out with shaking at 4 °C overnight. On day 2, sections were rinsed three times for 10 min in PBS and incubated for 90 min with a donkey anti-rabbit, and/or anti-goat Cy3-, or Cy5-coupled secondary antibody (Jackson ImmunoResearch, 1:500). Sections were rinsed three times for 10 min in PBS before mounting in PBS and coverslipped with Fluoromount.

#### 4.6. Images acquisition and analysis

Images were obtained from one set of brain sections (1/6th of the brain) for each immunostaining. For single stainings (DCX, c-Fos), brain regions of interest were identified at various Bregma coordinates. Images were acquired bilaterally with an epifluorescence microscope (Nikon) using a 10x objective. Quantifications were performed manually using an image analysis software (ImageJ 1.49v, NIH), taking into account cells with immunofluorescence above background. For dual immunostainings (c-Fos co-labeled with SST), z-stacks images were acquired bilaterally with a Nikon A1R Si confocal laser, a TiE inverted research microscope using a 20x objective. Images (1024 resolution) were acquired as 14 μM z-stacks with a step size of 2 μM. For c-Fos intensity in SST-expressing cells, we measured c-Fos immunoreactivity in SST cells and expressed the data as a percentage of background in the same field of view. All analyses were performed by an investigator blinded to treatment and/or genotype.

#### 4.7. Blinding

During testing, investigators were not blind to conditions. However, freezing behavior was analyzed using FreezeView softwares (Actimetrics, Wilmette, IL).

#### 4.8. Statistical analysis

No statistical methods were used to pre-determine sample sizes but our sample sizes are similar to those reported in previous publications [46]. Statistical analysis was carried out using GraphPad Prism v7 software. Data (means ± SEM) were analyzed using unpaired two-tailed Student's T-test, ordinary one-way ANOVA followed by Tukey's multiple comparisons test when appropriate (difference among means,  $P < 0.05$ ), mixed factor two-way ANOVA (repeated measures over time) followed by Bonferroni's multiple comparisons test when appropriate (only if interaction,  $P < 0.05$ ). Data distribution was assumed to be normal but this was not formally tested unless specified otherwise. Detailed statistical analyses can be found in supplementary Table 1. In any case, significance was set at  $P < 0.05$ .

#### Data exclusion

No data were excluded.

## Data availability

All data generated in this study are available from the Lead Contact without restriction. Further information and request for original data should be directed to and will be fulfilled by Amar Sahay (asahay@mgh.harvard.edu).

## CRediT authorship contribution statement

**Antoine Besnard:** Execution of experiments, co-conceptualization, Writing, Review and Editing. **Amar Sahay:** Co-conceptualization, Writing, Review and Editing, Provision and management of resources.

## Acknowledgements

A.B. acknowledges support from 2014 NARSAD Young Investigator Award, Bettencourt-Schueller Foundation, Philippe Foundation and 2016 MGH ECOR Fund for Medical Discovery (FMD) Postdoctoral Fellowship Awards. A.S. acknowledges support from US National Institutes of Health Biobehavioral Research Awards for Innovative New Scientists (BRAINS) 1-R01MH104175, NIH-NIA 1R01AG048908-01A1, NIH 1R01MH111729-01, NINDS R56NS117529, the James and Audrey Foster MGH Research Scholar Award, Ellison Medical Foundation New Scholar in Aging, Whitehall Foundation, the Inscopix Decode Award, the NARSAD Independent Investigator Award, Ellison Family Philanthropic support, Blue Guitar Fund, Harvard Neurodiscovery Center/MADRC Center Pilot Grant Award, a Alzheimer's Association research grant, the Harvard Stem Cell Institute (HSCI) Development grant and a HSCI seed grant. A.S thanks L. M. Sahay for proof reading manuscript.

## Appendix A. Supplementary data

Supplementary material related to this article can be found, in the online version, at doi:<https://doi.org/10.1016/j.bbr.2020.112917>.

## References

- [1] J. Altman, G.D. Das, Autoradiographic and histological evidence of postnatal hippocampal neurogenesis in rats, *J. Comp. Neurol.* 124 (1965) 319–335.
- [2] K.L. Spalding, O. Bergmann, K. Alkass, S. Bernard, M. Salehpour, H.B. Huttner, E. Bostrom, I. Westerlund, C. Vial, B.A. Buchholz, et al., Dynamics of hippocampal neurogenesis in adult humans, *Cell* 153 (2013) 1219–1227.
- [3] M. Boldrini, C.A. Fulmore, A.N. Tartt, L.R. Simeon, I. Pavlova, V. Poposka, G. B. Rosokljica, A. Stankov, V. Arango, A.J. Dwork, et al., Human hippocampal neurogenesis persists throughout aging, *Cell Stem Cell* 22 (2018) 589–599, e585.
- [4] E.P. Moreno-Jimenez, M. Flor-Garcia, J. Terreros-Roncal, A. Rabano, F. Cafini, N. Pallas-Bazarra, J. Avila, M. Llorens-Martin, Adult hippocampal neurogenesis is abundant in neurologically healthy subjects and drops sharply in patients with Alzheimer's disease, *Nat. Med.* 25 (2019) 554–560.
- [5] S.M. Miller, A. Sahay, Functions of adult-born neurons in hippocampal memory interference and indexing, *Nat. Neurosci.* 22 (2019) 1565–1575.
- [6] S.F. Sorrells, M.F. Paredes, A. Cebrían-Silla, K. Sandoval, D. Qi, K.W. Kelley, D. James, S. Mayer, J. Chang, K.I. Auguste, et al., Human hippocampal neurogenesis drops sharply in children to undetectable levels in adults, *Nature* 555 (2018) 377–381.
- [7] C. Zhao, W. Deng, F.H. Gage, Mechanisms and functional implications of adult neurogenesis, *Cell* 132 (2008) 645–660.
- [8] N. Toni, A.F. Schinder, Maturation and functional integration of new granule cells into the adult Hippocampus, *Cold Spring Harb. Perspect. Biol.* 8 (2015), a018903.
- [9] J.B. Aimone, Y. Li, S.W. Lee, G.D. Clemenson, W. Deng, F.H. Gage, Regulation and function of adult neurogenesis: from genes to cognition, *Physiol. Rev.* 94 (2014) 991–1026.
- [10] K.M. Christian, H. Song, G.L. Ming, Functions and dysfunctions of adult hippocampal neurogenesis, *Annu. Rev. Neurosci.* 37 (2014) 243–262.
- [11] D. Berron, H. Schutze, A. Maass, A. Cardenas-Blanco, H.J. Kuijff, D. Kumaran, E. Duzel, Strong evidence for pattern separation in human dentate gyrus, *J. Neurosci.* 36 (2016) 7569–7579.
- [12] A. Besnard, A. Sahay, Adult hippocampal neurogenesis, fear generalization, and stress, *Neuropsychopharmacology* 41 (2016) 24–44.
- [13] W. Deng, M. Mayford, F.H. Gage, Selection of distinct populations of dentate granule cells in response to inputs as a mechanism for pattern separation in mice, *eLife* 2 (2013), e00312.
- [14] H. Lee, C. Wang, S.S. Deshmukh, J.J. Knierim, Neural population evidence of functional heterogeneity along the CA3 transverse Axis: pattern completion versus pattern separation, *Neuron* 87 (2015) 1093–1105.
- [15] J.K. Leutgeb, S. Leutgeb, M.B. Moser, E.I. Moser, Pattern separation in the dentate gyrus and CA3 of the hippocampus, *Science* 315 (2007) 961–966.
- [16] A.D. Madar, L.A. Ewell, M.V. Jones, Temporal pattern separation in hippocampal neurons through multiplexed neural codes, *PLoS Comput. Biol.* 15 (2019), e1006932.
- [17] A.D. Madar, L.A. Ewell, M.V. Jones, Pattern separation of spiketrains in hippocampal neurons, *Sci. Rep.* 9 (2019) 5282.
- [18] J.P. Neunuebel, J.J. Knierim, CA3 retrieves coherent representations from degraded input: direct evidence for CA3 pattern completion and dentate gyrus pattern separation, *Neuron* 81 (2014) 416–427.
- [19] J.J. Sakon, W.A. Suzuki, A neural signature of pattern separation in the monkey hippocampus, *Proc. Natl. Acad. Sci. U. S. A.* 116 (2019) 9634–9643.
- [20] N.I. Woods, F. Stefanini, D.L. Apodaca-Montano, I.M.C. Tan, J.S. Biane, M. A. Kheirbek, The dentate gyrus classifies cortical representations of learned stimuli, *Neuron* 107 (2020) 173–184, e176.
- [21] A. Sahay, K.N. Scobie, A.S. Hill, C.M. O'Carroll, M.A. Kheirbek, N.S. Burghardt, A. A. Fenton, A. Dranovsky, R. Hen, Increasing adult hippocampal neurogenesis is sufficient to improve pattern separation, *Nature* 472 (2011) 466–470.
- [22] K.M. McAvoy, K.N. Scobie, S. Berger, C. Russo, N. Guo, P. Decharatanachart, H. Vega-Ramirez, S. Mlake-Lye, M. Whalen, M. Nelson, et al., Modulating neuronal competition dynamics in the Dentate Gyrus to rejuvenate aging memory circuits, *Neuron* 91 (2016) 1356–1373.
- [23] G. Berdugo-Vega, G. Arias-Gil, A. Lopez-Fernandez, B. Artegiani, J. M. Wasielewska, C.C. Lee, M.T. Lippert, G. Kempermann, K. Takagaki, F. Calegari, Increasing neurogenesis refines hippocampal activity rejuvenating navigational learning strategies and contextual memory throughout life, *Nat. Commun.* 11 (2020) 135.
- [24] E. Taha, S. Patil, I. Barrera, J. Panov, M. Khamaisi, C.G. Proud, C.R. Bramham, K. Rosenblum, eEF2/eEF2K pathway in the mature dentate gyrus determines neurogenesis level and cognition, *Curr. Biol.* (2020).
- [25] T. Nakashiba, J.D. Cushman, K.A. Pelkey, S. Renaudineau, D.L. Buhl, T.J. McHugh, V. Rodriguez Barrera, R. Chittajallu, K.S. Iwamoto, C.J. McBain, et al., Young dentate granule cells mediate pattern separation, whereas old granule cells facilitate pattern completion, *Cell* 149 (2012) 188–201.
- [26] N.B. Danielson, P. Kaifosh, J.D. Zaremba, M. Lovett-Barron, J. Tsai, C.A. Denny, E. M. Balough, A.R. Goldberg, L.J. Drew, R. Hen, et al., Distinct contribution of adult-born hippocampal granule cells to context encoding, *Neuron* 90 (2016) 101–112.
- [27] Y. Niibori, T.S. Yu, J.R. Epp, K.G. Akers, S.A. Josselyn, P.W. Frankland, Suppression of adult neurogenesis impairs population coding of similar contexts in hippocampal CA3 region, *Nat. Commun.* 3 (2012) 1253.
- [28] M.S. Fanselow, H.W. Dong, Are the dorsal and ventral hippocampus functionally distinct structures? *Neuron* 65 (2010) 7–19.
- [29] B.A. Strange, M.P. Witter, E.S. Lein, E.I. Moser, Functional organization of the hippocampal longitudinal axis, *Nat. Rev. Neurosci.* 15 (2014) 655–669.
- [30] D.M. Bannerman, R. Sprengel, D.J. Sanderson, S.B. McHugh, J.N. Rawlins, H. Monyer, P.H. Seeburg, Hippocampal synaptic plasticity, spatial memory and anxiety, *Nat. Rev. Neurosci.* 15 (2014) 181–192.
- [31] P.W. Frankland, V. Cestari, R.K. Filipkowski, R.J. McDonald, A.J. Silva, The dorsal hippocampus is essential for context discrimination but not for contextual conditioning, *Behav. Neurosci.* 112 (1998) 863–874.
- [32] M.A. Kheirbek, L.J. Drew, N.S. Burghardt, D.O. Costantini, L. Tannenholz, S. E. Ahmari, H. Zeng, A.A. Fenton, R. Hen, Differential control of learning and anxiety along the dorsoventral axis of the dentate gyrus, *Neuron* 77 (2013) 955–968.
- [33] S. Cioocchi, J. Passecker, H. Malagon-Vina, N. Mikus, T. Klausberger, Brain computation. Selective information routing by ventral hippocampal CA1 projection neurons, *Science* 348 (2015) 560–563.
- [34] J.C. Jimenez, K. Su, A.R. Goldberg, V.M. Luna, J.S. Biane, G. Ordek, P. Zhou, S. K. Ong, M.A. Wright, L. Zweifel, et al., Anxiety cells in a hippocampal-hypothalamic circuit, *Neuron* 97 (2018) 670–683, e676.
- [35] N.A. Cayco-Gajic, R.A. Silver, Re-evaluating circuit mechanisms underlying pattern separation, *Neuron* 101 (2019) 584–602.
- [36] T. Hainmueller, M. Bartos, Dentate gyrus circuits for encoding, retrieval and discrimination of episodic memories, *Nat. Rev. Neurosci.* 21 (2020) 153–168.
- [37] V.M. Luna, C. Anacker, N.S. Burghardt, H. Khandaker, V. Andreu, A. Millette, P. Leary, R. Ravenelle, J.C. Jimenez, A. Mastrodonato, et al., Adult-born hippocampal neurons bidirectionally modulate entorhinal inputs into the dentate gyrus, *Science* 364 (2019) 578–583.
- [38] C.L. Thompson, S.D. Pathak, A. Jeromin, L.L. Ng, C.R. MacPherson, M.T. Mortrud, A. Cusick, Z.L. Riley, S.M. Sunkin, A. Bernard, et al., Genomic anatomy of the hippocampus, *Neuron* 60 (2008) 1010–1021.
- [39] I. Fernandez-Lamo, D. Gomez-Dominguez, A. Sanchez-Aguilera, A. Oliva, A. V. Morales, M. Valero, E. Cid, A. Berenyi, L. Menendez de la Prida, Proximodistal organization of the CA2 hippocampal area, *Cell Rep.* 26 (2019) 1734–1746, e1736.
- [40] E.J. Henriksen, L.L. Colgin, C.A. Barnes, M.P. Witter, M.B. Moser, E.I. Moser, Spatial representation along the proximodistal axis of CA1, *Neuron* 68 (2010) 127–137.
- [41] M.S. Cembrowski, J.L. Bachman, L. Wang, K. Sugino, B.C. Shields, N. Spruston, Spatial gene-expression gradients underlie prominent heterogeneity of CA1 pyramidal neurons, *Neuron* 89 (2016) 351–368.
- [42] Y. Nakazawa, A. Pevzner, K.Z. Tanaka, B.J. Wiltgen, Memory retrieval along the proximodistal axis of CA1, *Hippocampus* 26 (2016) 1140–1148.

- [43] T.D. Goode, K.Z. Tanaka, A. Sahay, T.J. McHugh, An integrated index: engrams, place cells, and hippocampal memory, *Neuron* (2020).
- [44] A.H. Luo, P. Tahsili-Fahadan, R.A. Wise, C.R. Lupica, G. Aston-Jones, Linking context with reward: a functional circuit from hippocampal CA3 to ventral tegmental area, *Science* 333 (2011) 353–357.
- [45] A. Besnard, Y. Gao, M. TaeWoo Kim, H. Twarkowski, A.K. Reed, T. Langberg, W. Feng, X. Xu, D. Saur, L.S. Zweifel, et al., Dorsolateral septum somatostatin interneurons gate mobility to calibrate context-specific behavioral fear responses, *Nat. Neurosci.* 22 (2019) 436–446.
- [46] A. Besnard, S.M. Miller, A. Sahay, Distinct dorsal and ventral hippocampal CA3 outputs govern contextual fear discrimination, *Cell Rep.* 30 (2020) 2360–2373, e2365.
- [47] I. Imayoshi, M. Sakamoto, T. Ohtsuka, K. Takao, T. Miyakawa, M. Yamaguchi, K. Mori, T. Ikeda, S. Itoharu, R. Kageyama, Roles of continuous neurogenesis in the structural and functional integrity of the adult forebrain, *Nat. Neurosci.* 11 (2008) 1153–1161.
- [48] K.G. Akers, A. Martinez-Canabal, L. Restivo, A.P. Yiu, A. De Cristofaro, H.L. Hsiang, A.L. Wheeler, A. Guskjolen, Y. Niibori, H. Shoji, et al., Hippocampal neurogenesis regulates forgetting during adulthood and infancy, *Science* 344 (2014) 598–602.
- [49] M. Arruda-Carvalho, M. Sakaguchi, K.G. Akers, S.A. Josselyn, P.W. Frankland, Posttraining ablation of adult-generated neurons degrades previously acquired memories, *J. Neurosci.* 31 (2011) 15113–15127.
- [50] T. Ikrar, N. Guo, K. He, A. Besnard, S. Levinson, A. Hill, H.K. Lee, R. Hen, X. Xu, A. Sahay, Adult neurogenesis modifies excitability of the dentate gyrus, *Front. Neural Circuits* 7 (2013) 204.
- [51] S.A. Josselyn, S. Tonegawa, Memory engrams: recalling the past and imagining the future, *Science* (2020) 367.
- [52] C. Anacker, V.M. Luna, G.S. Stevens, A. Millette, R. Shores, J.C. Jimenez, B. Chen, R. Hen, Hippocampal neurogenesis confers stress resilience by inhibiting the ventral dentate gyrus, *Nature* 559 (2018) 98–102.
- [53] T. van Groen, P. Miettinen, I. Kadish, The entorhinal cortex of the mouse: organization of the projection to the hippocampal formation, *Hippocampus* 13 (2003) 133–149.
- [54] S. Ohara, S. Sato, K. Tsutsui, M.P. Witter, T. Iijima, Organization of multisynaptic inputs to the dorsal and ventral dentate gyrus: retrograde trans-synaptic tracing with rabies virus vector in the rat, *PLoS One* 8 (2013), e78928.
- [55] T. Nakashiba, J.Z. Young, T.J. McHugh, D.L. Buhl, S. Tonegawa, Transgenic inhibition of synaptic transmission reveals role of CA3 output in hippocampal learning, *Science* 319 (2008) 1260–1264.
- [56] K.B. Kjelstrup, T. Solstad, V.H. Brun, T. Hafting, S. Leutgeb, M.P. Witter, E.I. Moser, M.B. Moser, Finite scale of spatial representation in the hippocampus, *Science* 321 (2008) 140–143.
- [57] P.K. Cullen, T.L. Gilman, P. Winiecki, D.C. Riccio, A.M. Jasnow, Activity of the anterior cingulate cortex and ventral hippocampus underlie increases in contextual fear generalization, *Neurobiol. Learn. Mem.* 124 (2015) 19–27.
- [58] S. Ortiz, M.S. Latsko, J.L. Fouty, S. Dutta, J.M. Adkins, A.M. Jasnow, Anterior cingulate cortex and ventral hippocampal inputs to the basolateral amygdala selectively control generalized fear, *J. Neurosci.* 39 (2019) 6526–6539.
- [59] A.T. Keinath, M.E. Wang, E.G. Wann, R.K. Yuan, J.T. Dudman, I.A. Muzzio, Precise spatial coding is preserved along the longitudinal hippocampal axis, *Hippocampus* 24 (2014) 1533–1548.
- [60] S. Maren, K.L. Phan, I. Liberzon, The contextual brain: implications for fear conditioning, extinction and psychopathology, *Nat. Rev. Neurosci.* 14 (2013) 417–428.
- [61] T. Raam, K.M. McAvoy, A. Besnard, A.H. Veenema, A. Sahay, Hippocampal oxytocin receptors are necessary for discrimination of social stimuli, *Nat. Commun.* 8 (2017) 2001.
- [62] Q. Sun, A. Sotayo, A.S. Cazzulino, A.M. Snyder, C.A. Denny, S.A. Siegelbaum, Proximodistal heterogeneity of hippocampal CA3 pyramidal neuron intrinsic properties, connectivity, and reactivation during memory recall, *Neuron* 95 (2017) 656–672, e653.
- [63] M.R. Hunsaker, J.S. Rosenberg, R.P. Kesner, The role of the dentate gyrus, CA3a,b, and CA3c for detecting spatial and environmental novelty, *Hippocampus* 18 (2008) 1064–1073.
- [64] R.P. Kesner, A process analysis of the CA3 subregion of the hippocampus, *Front. Cell. Neurosci.* 7 (2013) 78.
- [65] D.F. Marrone, E. Satvat, I.V. Odintsova, A. Gheidi, Dissociation of spatial representations within hippocampal region CA3, *Hippocampus* 24 (2014) 1417–1420.
- [66] P.A. Naber, F.H. Lopes da Silva, M.P. Witter, Reciprocal connections between the entorhinal cortex and hippocampal fields CA1 and the subiculum are in register with the projections from CA1 to the subiculum, *Hippocampus* 11 (2001) 99–104.
- [67] Y. Sun, D.A. Nitz, T.C. Holmes, X. Xu, Opposing and complementary topographic connectivity gradients revealed by quantitative analysis of canonical and noncanonical hippocampal CA1 inputs, *eNeuro* (2018) 5.
- [68] B.J. Claiborne, D.G. Amaral, W.M. Cowan, A light and electron microscopic analysis of the mossy fibers of the rat dentate gyrus, *J. Comp. Neurol.* 246 (1986) 435–458.
- [69] M.P. Witter, Intrinsic and extrinsic wiring of CA3: indications for connectional heterogeneity, *Learn. Mem.* 14 (2007) 705–713.
- [70] I. Galimberti, E. Bednarek, F. Donato, P. Caroni, EphA4 signaling in juveniles establishes topographic specificity of structural plasticity in the hippocampus, *Neuron* 65 (2010) 627–642.
- [71] N.H. Nakamura, V. Flasbeck, N. Maingret, T. Kitsukawa, M.M. Sauvage, Proximodistal segregation of nonspatial information in CA3: preferential recruitment of a proximal CA3-distal CA1 network in nonspatial recognition memory, *J. Neurosci.* 33 (2013) 11506–11514.
- [72] A.N. Opalka, D.V. Wang, Hippocampal efferents to retrosplenial cortex and lateral septum are required for memory acquisition, *Learn. Mem.* 27 (2020) 310–318.
- [73] K.Z. Tanaka, H. He, A. Tomar, K. Niisato, A.J.Y. Huang, T.J. McHugh, The hippocampal engram maps experience but not place, *Science* 361 (2018) 392–397.
- [74] K. Ghandour, N. Ohkawa, C.C.A. Fung, H. Asai, Y. Saitoh, T. Takekawa, R. Okubo-Suzuki, S. Soya, H. Nishizono, M. Matsuo, et al., Orchestrated ensemble activities constitute a hippocampal memory engram, *Nat. Commun.* 10 (2019) 2637.
- [75] A. Besnard, S. Laroche, J. Caboche, Comparative dynamics of MAPK/ERK signalling components and immediate early genes in the hippocampus and amygdala following contextual fear conditioning and retrieval, *Brain Struct. Funct.* 219 (2014) 415–430.
- [76] O. Takeuchi, J. Fisher, H. Suh, H. Harada, B.A. Malynn, S.J. Korsmeyer, Essential role of BAX, BAK in B cell homeostasis and prevention of autoimmune disease, *Proc. Natl. Acad. Sci. U. S. A.* 102 (2005) 11272–11277.